EFDA–JET–R(13)03

ITPA transport and confinement topical group and
ITPA pedestal and edge physics topical group

Joint Report on Analysis of ITER Divertor Strategy Final Report (v2.2) 30 April, 2013

Joint Report on Analysis of ITER Divertor Strategy Final Report (v2.2) 30 April, 2013

ITPA transport and confinement topical group and
ITPA pedestal and edge physics topical group

1. Introduction

The original strategy for the ITER divertor in ITER research plan in 2008 was that the replacement of CFC/W divertor with all W divertor during D-phase after the demonstration of a 15MA H-mode integrated scenario with ELM amelioration. In 2009, in order to accelerate initial operation phases before DT-phase, baseline strategy was revised that ITER operation starts with CFC/W divertor and it changes out to full W divertor before the nuclear phase (D-phase) after the confirmation of the controllability of transient events in H/He phase. However, in the frame of the ITER cost containment policy, the option for implementing a single divertor up to achieving the Q=10 milestone in the nuclear phase has been proposed by ITER organization and supported by ITER council. Then, the ITPA Coordinating Committee has asked the ITPA groups to provide a scientific view on issues linked with the ITER divertor strategy for submission to ITER Science and Technology Advisory Committee held in May 2013.

In ITPA “transport and confinement (T&C) topical group” and “pedestal and edge physics (PEP) topical group”, joint session discussing ITER divertor strategy at autumn meeting held in San Diego, October 2012. In the session, influence of W divertor on the access to the H-mode, effect of W divertor on pedestal parameters and plasma confinement, predicted impacts of wall and divertor material on pedestal structure, requirements for ELM control to prevent W accumulation, transport of high Z impurities in the core plasma and possibilities for its control have been discussed. Based on this session, both groups have agreed to provide joint report based on the common understanding that no significant issue is identified in the T&C and PEP research area regarding the start of operations with a CFC/W divertor.

In this report, therefore, the evaluation has focused on the additional risks associated with the start of ITER operation up to the DT phase with a single W divertor, and has been structured in the following five topics:

1. Operation in L-mode (C. Angioni, M. Reinke)
2. Access to H-mode (J.W. Hughes, F. Ryter, C. Maggi)
3. Operation in H-mode (T. Pütterich, C. Angioni, R. Dux, V. Bobkov)
4. Quality of H-mode plasmas (M. Beurskens, J. Schweinzer, F. Ryter, M. Reinke)
5. Specific issues in He plasma operation (M. Reinke, C. Angioni, F. Ryter)

All assessment in this report is only valid if all diagnostics required for the safe operation in the initial phase are available and commissioned from the first plasma of ITER. The minimum set of diagnostics required for non-nuclear phase are listed in Table 3.2-1 in ITER Research Plan (v.2.2, IDM UID 2FB8AC)

Executive summary

Robust, stable L-mode operation of tokamaks with fully high-Z divertors has been demonstrated by a number of experiments around the world including ASDEX Upgrade (AUG), Alcator C-Mod and JET. The concentration levels of impurities from high-Z PFCs remains low in L-mode, without special requirements to control impurity accumulation, and below the limits compatible with ITER operation. At least for the properties of the plasma in the closed field line region, a W divertor in ITER is expected to be completely compatible with operation in L-mode.

As for the access to H-mode plasmas, comparisons among devices of H-mode power threshold, P_{L-H}, in D plasmas, and comparisons on single devices of P_{L-H} in D vs. He plasmas from all three devices suggest that ITER is not expected to have more challenging access to H-mode with a full W divertor than it would have with a C divertor. Experiments comparing P_{L-H} in D and He plasmas in JET, with its ITER-like wall, would be extremely valuable in making these conclusions firmer.

The recipes that have been developed in three devices, for controlling the heavy impurity content of the plasma are the maximization of local core heating, the control of the impurity penetration by ELM pace-making, deuterium puffing and the mitigation of erosion by impurity seeding. These recipes are expected to be effective also in ITER to ensure stable H-mode operation. Thus, the large mix of different heating systems, fuel and impurity gas valves and means of ELM control can be expected to allow successful H-mode operation also in ITER, in the nuclear and the non-nuclear phase. More specifically, in the non-nuclear phase, the early availability of the ECH system is recommended, since it has been proven to be a very effective tool.

The clearest difference seen between full Carbon and full metal devices is the loss of the well performing zero gas flux, low recycling scenario going from C to W or Be/W, especially for initial operation phase in ITER. However, in Q=10 scenario with high gas rates and/or pellet injection for heat load mitigation and for operation close to the density limit, this is of little consequence for the choice in divertor material. The use of low-Z impurity seeding may aid the baseline H-mode scenario in ITER with a full metal wall, especially for the high-δ plasmas. This is in good synergy with the need for divertor heat load mitigation.

Several uncertainties still limit the possibility of making precise predictions in the definition of scenarios in the pre-nuclear operation phase of ITER in He. However, the present knowledge allows us to conclude that there is no specific element connected with operation in He plasmas by which it should be expected that pre-nuclear operation in He could be severely hampered or even made impossible in the presence of a W divertor in ITER. One possible concern is an increase of hydrogen content in He plasma by hydrogen pellet injection for heavy impurity control, where the required power for L-H transition, P_{L-H}, can be increased.

2. Operation in L-mode

2.1 Introduction

As any other tokamak, ITER will start its operation in the low confinement mode (L-mode). In addition, early and late phases of any plasma discharge are in L-mode, before the heating power is increased in order to enter the high confinement mode (H-mode) and achieve the high performance phase, and after this phase, to end smoothly the plasma discharge. During the initial phase of ITER operation in L-mode, many systems, including the heating systems, are commissioned. Therefore, an important requirement is that L-mode plasma operation (including Ohmic L-mode operation) is reliably stable. This implies that in ITER, in the presence of a W divertor, L-mode operation should not require special external means to control W accumulation.

In this section, the main observations on the behaviour of high-Z impurities in L-mode plasmas (including Ohmic plasmas) with metallic plasma facing components are reviewed, and conclusions are drawn on the potential impact of a full W divertor on L-mode operation in ITER. In section 2.2 we briefly review the dependence of the W cooling factor as a function of the electron temperature, and we emphasize that above 2 keV it becomes a decreasing function of increasing T_e, which is a good property for the high temperatures which will be achieved in ITER. In Section 2.3 the properties of impurity transport in L-mode plasmas with respect to other confinement modes and the behaviour of L-mode plasmas during the current flat top in high-Z PCFs devices are briefly reviewed. The general observation is that L-mode operation can be regularly performed without the need of any external mean for controlling W accumulation. In section 2.4 the behaviour of L-mode plasmas during current ramps is specifically examined.

2.2 W cooling factor and L-mode response to core radiation

Temperatures in ITER will be higher than in present devices. Therefore, the first element to consider is to examine how the power radiated by W depends on the electron temperature. The parameter which can be considered to this purpose is the cooling factor, $C(T_e)$ that is, the ratio of the radiated power per unit volume, ε, to the product of the electron and the impurity densities, with $\varepsilon=n_Z n_e C(T_e)$. The dependence of the tungsten cooling factor, C_W, as a function of the electron temperature is presented in Fig. 2.1, from Ref. [*Puetterich NF 10*]. As shown by the dashed blue and black lines, the C_W decreases above 2 keV and is reduced by one order of magnitude around 40 keV, despite of the increase of the Bremsstrahlung contribution to the total radiation. At 2.3 keV, C_W has been measured by experiments in ASDEX Upgrade (AUG), although with large uncertainties, and has been found in good agreement with the calculations. The dependence of the C_W as a function of T_e is favorable for operation at high temperatures like those expected in ITER.

The L-mode confinement scaling has been demonstrated to be independent of the core radiated power fraction, even up to P_{RAD}/P_{LOSS} approaching unity [*Greenwald FST*]. Using recycling, noble gases such as Ar, Kr and Xe enables radiative mantles to be formed, exhausting large fractions

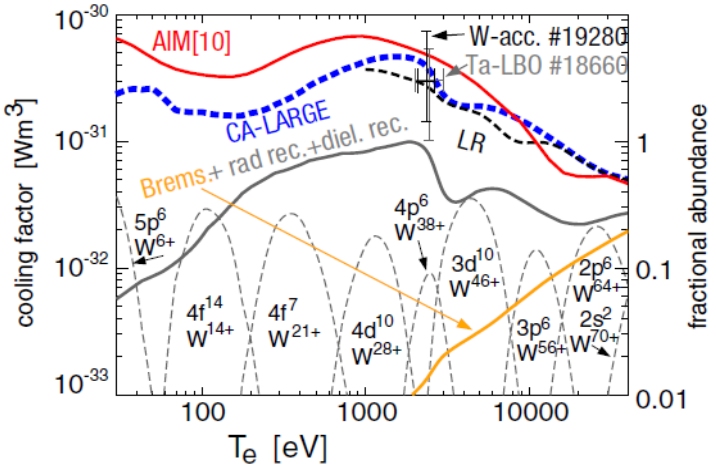

Figure 2.1 *(Fig. 2 of Ref. [Puetterich NF 10]) The total cooling factors of W from different models: AIM, Post et al Phys. Plasmas 2, 2328 (1995), level-resolved (LR) and configuration averaged (CA). The summed contributions due to radiative and dielectronic recombination and by Bremsstrahlung are presented with the grey solid curve. Fractional abundances for a few ionization stages are also presented.*

of the input power isotropically over a large area, reducing the burden on the divertor as we learn how to safely run ITER. This suggests robust L-mode operation of ITER with an all tungsten divertor will be possible during commissioning of high-power auxiliary systems with reduced risk of irreversible damage.

2.3 High-Z impurity transport and L-mode behaviour during current flat top

Several studies have been dedicated to investigate the transport of heavy impurities in different confinement regimes. In L-mode it is observed that the impurity confinement time is weakly dependent on the impurity charge [Marmar NF 82], is anomalously large and significantly shorter than in H-modes [Rice FST 07], as shown in Fig. 2.2. The confinement time of impurities increases as the energy confinement time increases. Measurements in the core show that impurity transport coefficients are anomalously large (above neoclassical levels) in the confinement region of L-mode plasmas [Carraro PPCF 04, Rice FST 07, Guirlet NF 09, Giroud ITPA 10, Sertoli PPCF 11, Howard PoP 12, Howard NF 12] and increase with increasing minor radius. All these properties are at least qualitatively consistent with impurity transport produced by turbulence, which is also predicted to become weakly dependent on Z at high-Z. First comparisons of gyrokinetic turbulent impurity transport predictions with experimental observations in L-mode find promising quantitative agreement [Howard NF 12]. Impurity transport near the magnetic axis can approach neoclassical levels [e.g. Guirlet NF 09], but is also observed to strongly increase in response to application of central auxiliary heating [Sertoli PPCF 11], similarly to observations in H-mode [section 4 and refs therein].

The main difference between impurity confinement in L-modes and in H-modes can be identified in the transport properties at the edge. In the H-mode pedestal impurity transport is observed

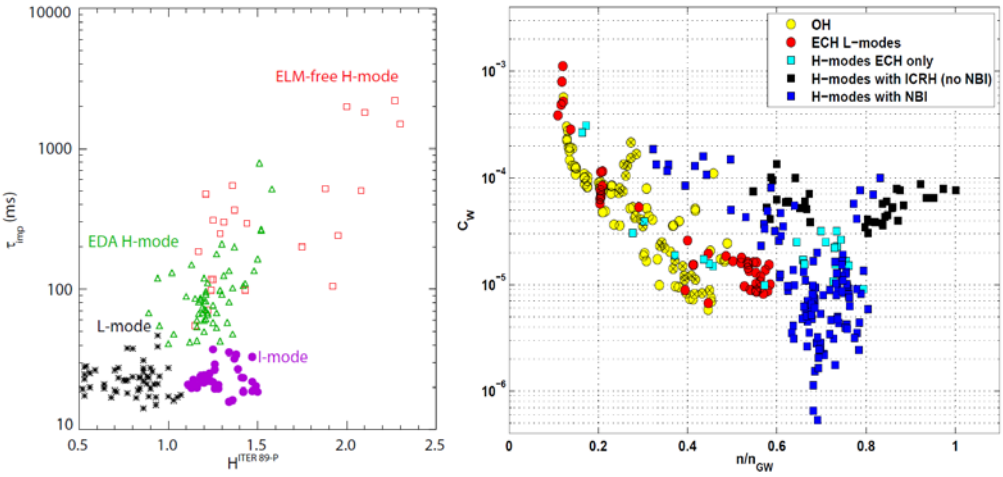

Figure 2.2 *(left, C-Mod Rice FST 2007). Impurity confinement time as a function of the H_{89} confinement factor in Alcator C-Mod experiments. L-mode has anomalously low values of impurity confinement time.* ***Figure 2.3*** *(right, AUG). W concentration in Ohmic heating (OH), L-mode and H-mode and with different auxiliary heating in ASDEX Upgrade. Crosses identify phases during current ramp-up*

to follow the neoclassical predictions [Puetterich JNM 11], whereas in L-mode it is dominated by turbulence. This interpretation is also consistent with observations in I-mode, where a pedestal in the main plasma density profile does not develop, in contrast to H-modes, and where impurity confinement times are measured to be as low as in L-mode, despite of the improved energy confinement [White NF 10].

Also as a consequence of these different transport properties, W concentrations in L-mode are observed to be in general lower than in H-modes at similar densities, as illustrated by AUG results in Fig. 2.3, with additional variation due to auxiliary heating. In particular, Ohmic plasmas exhibit very low values of W concentration, at least if the density is sufficiently large, despite no means of controlling accumulation is applied in the discharge. The W concentrations increase with decreasing density, due to increased sputtering yields at higher temperatures and reduced dilution effects. Similar trends are observed also at JET [Groth, Coenen Priv. Comm., in SOLDIV Chapter 4 by S. Brezinsek] and for Mo in C-Mod [Reinke Priv. Comm.]. However, these high W concentrations do not prevent the regular stable development of the plasma discharge, since the actual amount of radiated power remains limited and L-modes are stable to radiation, as discussed earlier. At sufficiently large densities, the observed levels of W concentration in OH operation in AUG can be as low as 6×10^{-6}, particularly after boronization, and anyway below the W concentration of ~ 4×10^{-5} which has been estimated compatible with ITER operation [Loarte Priv. Comm.]. AUG boronized walls should be considered more relevant for ITER projections, since ITER will have a Be limiter and not a full W limiter like AUG.

In present devices L-mode phase is also encountered transiently during H-L back-transitions, which can be induced by unbalancing the net power, either by a momentary increase in radiated or a

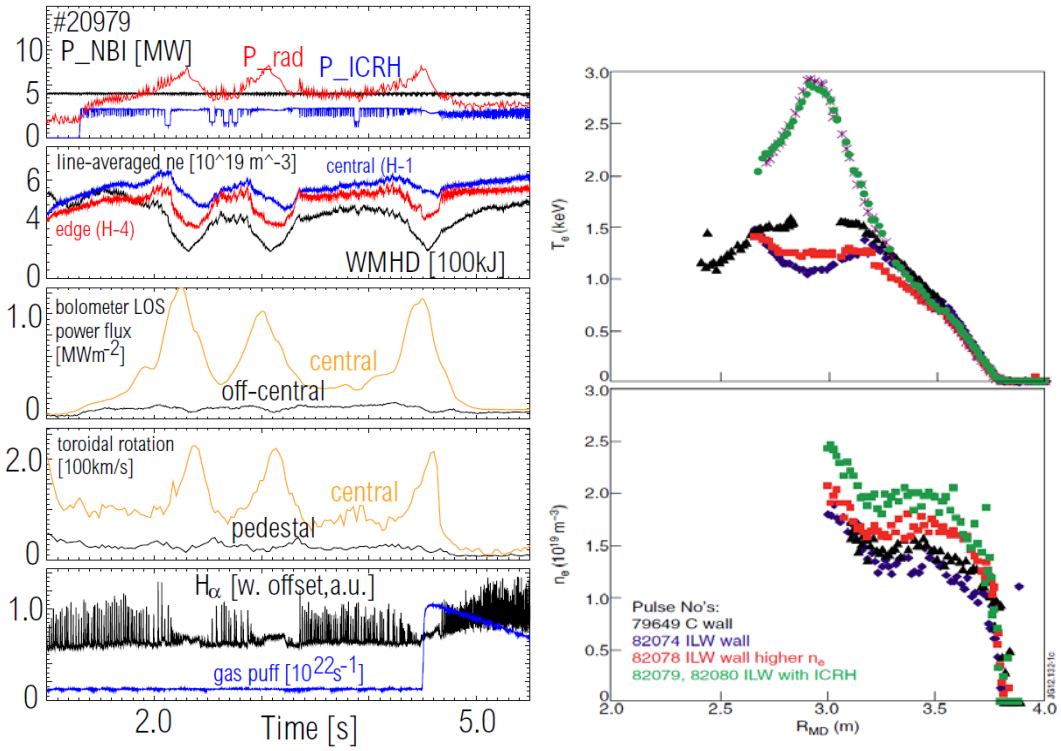

Figure 2.4 *(Left: AUG, Puetterich AUG Program seminar 2007) Time traces of the heating and radiated powers, of the central and peripheral line averaged densities and stored energy, of the line integrated radiated power density measured by central and peripheral lines of sight of a bolometer, central and edge plasma rotation, finally D-alpha signal and gas puff level. Repetitive transitions to L-mode take place as a consequence of increased central radiation.*
Figure 2.5 *(Right: JET, Mailloux EPS 2012, Fig. 1) Electron temperature and density profiles close to the end of the current ramp, contrasting C PFCs (black) with ILW at low density (red), ILW at higher density (blue), and ILW at higher density with the addition of ICRH (green and purple).*

drop out in heating power. Experiments show that even with enhanced core high-Z content, the H/L back-transition is stable and non-disruptive when triggered by on-axis accumulation. An example of this is shown for AUG in Fig. 2.4. During an H-mode phase without gas puff and both NBI and ICRF heating kept at constant power, the central accumulation of W and consequent central radiation leads to the loss of the H-mode. During the L-mode phase the radiated power suddenly drops (at the same zero gas puff and heating levels) which allows a new transition to H-mode. The cycle can be repeated multiple times, until an increase of the gas puff level allows the H-mode to be maintained stable, mainly by increasing the ELM frequency [see Section 4]. Similar behaviors of repetitive non-disruptive transition to L-mode as a consequence of excessive radiation due to central accumulation have been observed also in C-Mod and JET [ITPA Mtg 2012, San Diego]. These experimental results demonstrate generic good properties of L-mode in keeping low levels of high-Z impurities originated from metallic PFCs, even without applying any external mean to control impurity accumulation.

In contrast to these observations, some H-L transitions at JET were followed by a too long

residence of high Z impurities, producing excessive radiation in the core and leading to a radiation collapse [Joffrin, private communication: need Reference if available, and/or need to characterize these discharges with respect to those where this is not observed, e.g. is it too low power]. Also in these JET cases, the application of ICRH was observed to be beneficial to reduce the W accumulation and increase the electron temperature (also reducing the cooling factor). These observations identify the need of appropriate operation to smoothly produce the H-L back-transition in the last phase of the plasma discharge, likely keeping sufficient levels of central heating and gas puff.

2.4 High-Z impurity behaviour in L-mode during current ramps

An important aspect of L-mode operation is during current ramps. In addition to aspects related to plasma-wall interaction, there are several features which imply that during current ramps the core plasma can behave differently with high-Z PFCs with respect to C PFCs. An important aspect, for instance, is the lower value of the effective charge with tungsten PFCs, leading to a lower resistivity and a longer time for the penetration of the plasma current. In addition, during the early phase of the current ramp up, particularly in the presence of concomitant low values of plasma density, relatively high values of W concentration can be present in the plasma and effects of strong central radiation have been observed in FTU [Buratti PPCF 97], JET [Mailloux EPS 2012], and AUG [Fietz NF in print]. An example from JET [Mailloux EPS 2012] is presented in Fig. 2.5, where hollow temperature profiles develop during a current ramp at low density. The effect can be mitigated with increased levels of gas puff and/or with the application of central heating (central ICRH in this case). While the development of centrally hollow temperature profiles during the current ramp-up does not prevent the stable evolution of the plasma discharge, this has the consequence of centrally reversed shapes of the current density and safety factor profiles during the current ramp and at the beginning of the flat-top phase. These features can impact the development of the high power phase of the discharge scenario, and have to be taken into account. Also in AUG centrally hollow T_e profiles have been observed during current ramps in the case of non-boronized W walls (where also low-Z impurities are abundant), whereas centrally peaked T_e profiles have been observed during current ramps with boronized W walls [Fietz NF 2012]. As already mentioned, the latter condition can be considered more relevant for ITER, which will have a Be limiter, in contrast with the full W limiter in AUG. With boronized W walls in AUG, the W concentration during the current ramp of typical 1 MA plasmas is usually around 2×10^{-4} during the early limited phase and it is suddenly reduced to 1×10^{-4} at the formation of the X-point (current below 0.4 MA, $n/n_{GW} \sim 0.25$). During the consequent remaining phase of the current ramp up and the raise of the plasma density, the W concentration quickly drops to reach levels below 10^{-5} at the end of the ramp ($n/n_{GW} \sim 0.5$) [Fig. 2.3]. In addition, in ITER these effects might be in any case reduced due to the expected higher values of the electron temperature, and the reduced values of cooling factors with respect to JET and AUG.

2.5 Summary

Robust, stable L-mode operation of tokamaks with fully high-Z divertors has been demonstrated by a number of experiments around the world including AUG, Alcator C-Mod and JET. The concentration levels of impurities from high-Z PFCs remains low in L-mode, without special requirements to control impurity accumulation, and below the limits compatible with ITER operation. The transport of high-Z impurities is observed to be largely anomalous (turbulent), independent of the impurity charge, and increases with increasing minor radius. While the detailed understanding of heavy impurity transport in L-mode plasmas, dominated by turbulence in most conditions, remains limited, an increasing number of quantitative comparisons are being made between theoretical predictions and experimental measurements in the core and at the edge. An improved understanding would certainly be an important step forward, not only in the route towards the validation of turbulent transport models, but also for a more reliable design and prediction of the scenarios, particularly during transient phases like current and density ramps and confinement mode transitions.

Nevertheless, the present understanding, albeit limited, allows us to draw the above conclusions which are of particular relevance in the assessment of the impact of a W divertor to L-mode operation in ITER. On this basis, we conclude that, at least for the properties of the plasma in the closed field line region, a W divertor in ITER is expected to be completely compatible with operation in L-mode.

References

[Puetterich NF 10] T. Puetterich et al., Nucl. Fusion **50** (2010) 025012

[Greenwald FST] M. Greenwald et al., Fusion Sci. Technol. 51 (2007) 266

[Marmar NF 82] E.S. Marmar et al., Nucl. Fusion **22** (1982) 1567

[Rice FST 07] J.E. Rice et al., Fusion Sci. Technol. **51** (2007) 357

[Carraro PPCF 04] L. Carraro et al., Plasma Phys. Control. Fusion 46 (2004) 389

[Guirlet NF 09] R. Guirlet *et al., Nucl. Fusion* **49** (2010) 055007

[Giroud ITPA 2010] C. Giroud et al, ITPA Mtg of T&C Group 2010, Culham.

[Sertoli PPCF 2011] M. Sertoli et al., Plasma Phys. Control. Fusion **53** (2011) 035024.

[Howard PoP 2012] N. Howard et al., Phys. Plasmas **19** (2012) 056110

[Howard NF 2012] N. Howard et al., Nucl. Fusion **52** (2012) 063002

[White NF 10] D. White et al., Nucl. Fusion **50** (2010) 105005

[Puetterich JNM 11] T. Puetterich et al., J. Nucl. Mat. **415** (2011) S334

[Buratti PPCF 97] P. Buratti et al, Plasma Phys. Control. Fusion **39** (1997) B383

[Mailloux EPS 12] J. Mailloux et al, EPS Conf. on Plasma Physics, Stockholm (2012).

[Fietz NF 13] S. Fietz et al, Nucl Fusion (2013) in print.

3. Access to H-mode

3.1 Introduction

Three tokamaks have performed extensive studies of H-mode access in the presence of metal PFCs: Alcator C-Mod, ASDEX Upgrade (AUG) and JET. C-Mod has always operated with both first wall and divertor PFCs composed predominately of bulk molybdenum tiles, with and without boron surface coatings. AUG and JET both began with predominately carbon PFCs, then transitioned to metal. AUG now operates with a full tungsten wall, and JET has installed ITER-like PFCs composed of beryllium (first wall) and tungsten (divertor). Thus AUG and JET, using data from multiple run campaigns, can directly compare H-mode access with C walls to that with metal walls. C-Mod offers supporting information in the form of comparing high-Z PFCs with low-Z coated surfaces.

In the following discussion, $P_{L\text{-}H}$ refers to the loss power calculated for a given discharge at the L-H transition. This quantity is often normalized to the scaling law adopted by ITER: $P_{scaling} = 0.049\,\bar{n}_e{}^{0.72} B_T{}^{0.80} S^{0.94}$, with threshold power $P_{scaling}$ in MW, line-averaged density $\bar{n}_e$ in 10^{20}m^{-3}, toroidal field B_T in T, and plasma surface area S in m^2.

3.2 AUG: Carbon vs. tungsten

The transition from a C wall to a W wall occurred on AUG in roughly two phases. The main chamber surfaces were switched from 2001 to 2005, and the divertor transition occurred between 2006 and 2007. Because of the AUG practice of running an "H-mode standard shot" at the beginning of each run day, it is possible to track $P_{L\text{-}H}$ over time, and across changes to device configuration. The H-mode in this standard discharge is induced with NBI heating at a density which is significantly above the low-density branch of the power threshold. Fig. 3.1 shows the resultant $P_{L\text{-}H}$, normalized to that projected by the ITER scaling law, for a period of over a decade, in which W coverage increased from nearly zero to 100%. The most recent data, with full W coverage, show a distinct reduction in $P_{L\text{-}H}$ relative to the earlier data, with less than full coverage. Notably, the ~25% reduction in threshold power was only seen after full coverage (including the divertor surfaces) was obtained.

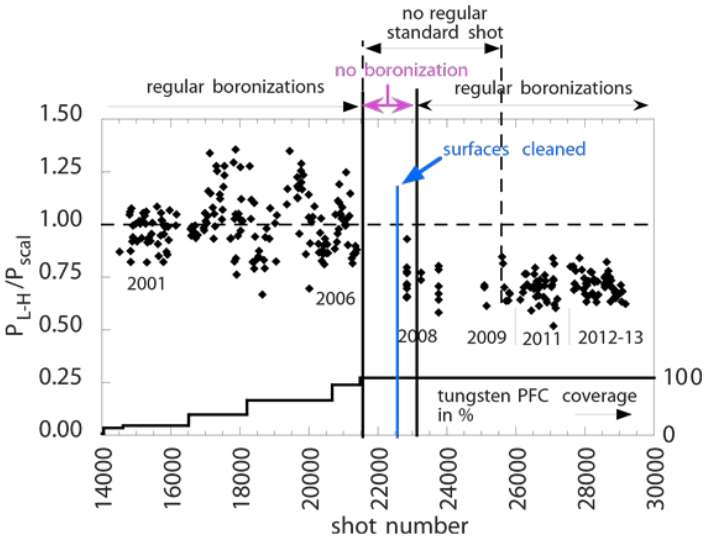

Figure 3.1 *Historical H-mode power threshold data on AUG, through changeover from C to W PFCs. [F. Ryter et al. submitted to Nucl. Fusion]*

H-mode threshold studies at other densities showed that the reduction in $P_{L\text{-}H}$ with W PFCs occurred for all

n_e>4x10^{19} m^{-3}, *i.e.* above the low-density branch for H-mode access. The quantitative effects of the C→W transition at low density cannot be assessed because of insufficient data from the C phase.

In addition, the W replacement had favorable effects on P_{L-H} in discharges fueled with isotopes other than D. The power threshold in H discharges was reduced in going from C to W, with P_{L-H}(H) remaining approximately equal to 1.8xP_{L-H}(D). The reduction of P_{L-H} in He discharges was actually more dramatic, since in studies with the C wall, P_{L-H}(He)=1.4xP_{L-H}(D), and with W, P_{L-H}(He)= P_{L-H}(D). As seen Fig. 3.2, P_{L-H} in both D and He are significantly below the ITER scaling law value for the W wall, provided AUG operates above the low-density branch for H-mode access. P_{L-H} in H discharges is above the scaling law projection, but only by about 30—40%.

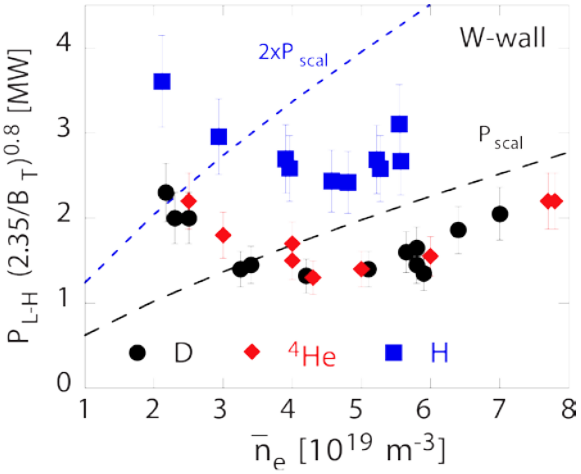

Figure 3.2 *Density dependence of H-mode power threshold data on AUG for D, H and He. Comparison to the ITER scaling law is shown. [F. Ryter et al. submitted to Nucl. Fusion]*

The cause of the reduction in P_{L-H} with W is not well understood. Both core radiation losses and edge neutral pressures have been evaluated in both C and W phases, and have not been found to differ within error bars. Edge electron temperature is on average lower, consistent with the reduced input power. A significant change is the C concentration, which after full W coverage was reduced from ~2% to ~0.5%.

3.3 JET: Carbon vs. beryllium/tungsten

In contrast to the gradual PFC transition on AUG, the switch from C to metal walls in JET was made entirely during one long torus opening. Effects on P_{L-H} were studied by repeating L-H experiments with the Be/W wall that had been performed with the C wall. These comparisons were done in D discharges with density variation, and employed both NBI- and ICRF-heating. Experiments with the ILW show significant changes in P_{L-H} are possible due to variations in plasma shaping and strike point placement. Therefore, to evaluate changes due to PFC composition, matched divertor geometry and plasma shaping were used in all direct comparisons, such as in Fig. 3.3. With C PFCs and the MkII-HD divertor, P_{L-H} was seen to be monotonic with density, and in very good agreement with the ITER scaling law. Introduction of Be/W PFCs resulted in the appearance of a local minimum in P_{L-H}(n_e) and a low-density branch with elevated power threshold. Such a minimum had been previously observed in JET with C PFCs, but in a divertor configuration with private flux zone septum (MkII-GB). This combined experience shows that the properties of the low-density branch can be

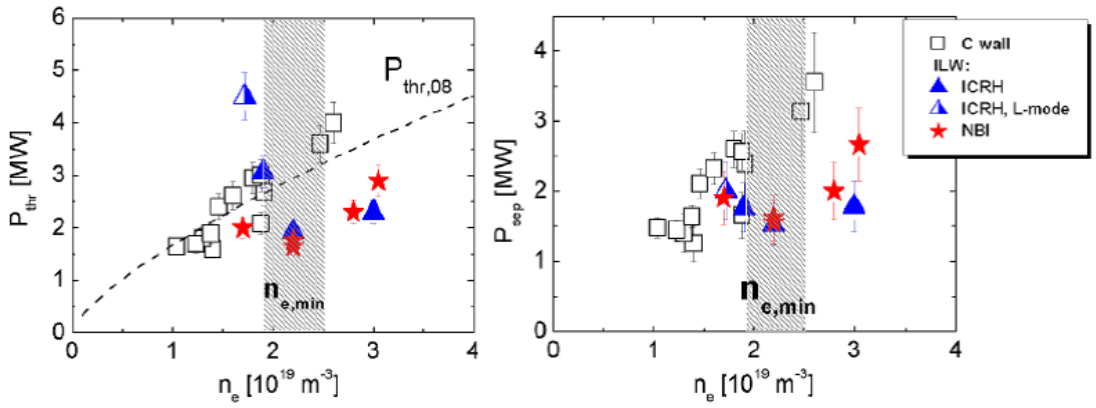

Figure 3.3 *Density dependence of H-mode power threshold data on JET with C MkII-HD (squares) and ILW (stars, triangles) divertors. Comparison to the ITER scaling law is shown. [C. Maggi, EPS 2012]*

significantly affected by both divertor geometry and material composition.

As on AUG, the transition from C to metals in fixed divertor geometry resulted in lower P_{L-H} for all but very low densities, with $P_{L-H}/P_{scaling}<1$ in many cases. The favorable reduction in P_{L-H} for $n_e>2x10^{19}$ m^{-3} is persistent for both NBI and ICRF-heated discharges. For lower densities, P_{L-H} appears less favorable for ICRF heated discharges than for those with NBI. This can be attributed to a strong increase in the fraction of power radiated in the core plasma when ICRF is used in the presence of W at low plasma density. When the L-H data are recast in terms of $P_{sep}=P_{L-H}-P_{rad,core}$, the ICRF and NBI data are found to overlay well. Still the power threshold expressed in this manner is lower than that in the C machine, at least when operating above the low-density branch.

For NBI-only discharges, L-mode core radiated power levels were not substantially different between C and Be/W campaigns. Radiation in the lower divertor, in the vicinity of the X-point, was slightly reduced for all cases with metal walls, relative to C walls. As on AUG, a reduction in edge T_e at L-H was observed following the transition from C to metal.

3.4 Interpretation

It is challenging to produce a physics-based explanation for the changes in P_{L-H} observed in AUG and JET. It has long been hypothesized that a critical E_r shear is needed to suppress L-mode turbulence and initiate the transition to H-mode. This implies that the H-mode threshold is sensitive to the local ion pressure profile and flows, quantities which are not uniformly measured across the data sets used in these studies. Also highly uncertain are the role of neutrals and the importance of the interaction between fluctuating flow fields (e.g. GAMs, zonal flows), mean flow and turbulence spectra.

Despite these uncertainties in the edge physics, there are remarkable similarities in the P_{L-H} observed across devices with all-metal PFCs (and in particular, high-Z divertor). All observe a minimum P_{L-H} at a specific optimum density $n_{L-H,opt}$, where $P_{L-H,min}$ is below the projection from the ITER scaling law. (This non-monotonic dependence on density has also been observed with C PFCs,

although not always as clearly. Transitioning from C to metal may accentuate the low-density P_{L-H} behavior by (a) decreasing P_{L-H} in the high density branch and (b) raising the density at which the low-density branch takes effect.) For completeness, C-Mod results are shown in Fig. 3.4.

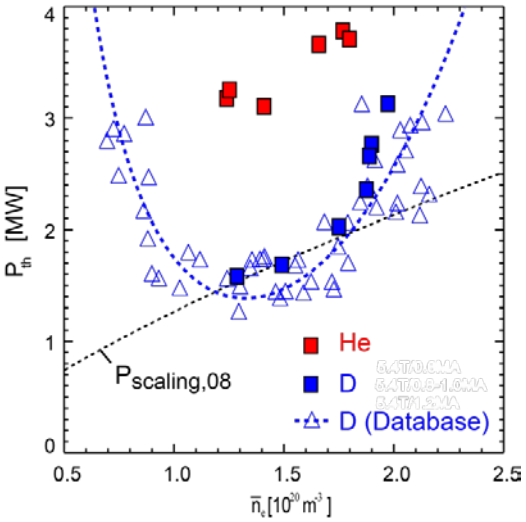

Figure 3.4 *H-mode power threshold on C-Mod from an extensive D database (triangles) and from a dedicated experiment to compare P_{th} in D and He (squares). Comparison to the ITER scaling law is shown. [Y. Ma, PhD Thesis, MIT (2012)]*

Combining observations from C-Mod, AUG and JET (including toroidal field scans on C-Mod and JET), one may conclude that $n_{L-H,opt}$ scales approximately with B_T/R. If this scaling is extrapolated, then the $n_{L-H,opt}$ for ITER would be approximately 2—3x10^{19} m^{-3}, which is below its expected L-mode target density. There is no evidence that C PFCs would increase this density, and may actually decrease it for fixed geometry. It is therefore likely that ITER will operate well above the low-density branch regardless of divertor material. This in turn could allow ITER to exploit the favorable influence of metal walls on P_{L-H} (i.e. >25% reduction) observed on AUG and JET.

3.5 Non-nuclear phase issues

While the AUG results discussed in Sec 3.2 are favorable for H-mode access in He with metal walls, one cannot be absolutely sure that the substantially improved P_{th} in He is entirely due to tungsten. As can be seen in Fig. 3.4, there are counter-indications from C-Mod, where with Mo PFCs P_{th} in He is higher than that in D by a factor of 1.6—2.0. See Sec. 6.2 for detail. More information on P_{L-H} in He would be highly desirable on JET in order to help resolve this issue. This would include repeating He H-modes previously obtained with C PFCs (in which P_{L-H} was not onerously high) using nearly identical plasma parameters and geometry.

3.6 A note on boronization

Boronization for wall conditioning is utilized both on C-Mod and AUG. In many cases boronization is critically important for reducing impurity accumulation in a developed H-mode. However, the impact on L-mode and the H-mode power threshold is less well studied. In both C-Mod and AUG, long vessel openings to air impact the start of subsequent plasma operations due to residual concentrations of oxygen and hydrogen. (Additionally, high-Z contaminants like Fe and Cu are problematic during the start of campaigns on C-Mod.) Power thresholds for H-mode tend to be high early in a campaign, likely due to both increased impurity content and high H/D ratio. This is

compounded further on C-Mod, since a low H/(H+D) ratio is critical to obtaining good ICRF heating efficiency. Initial boronizations in the early phases of a run campaign can be helpful in reducing H fractions and impurity concentrations in the L-mode phase, which appears to facilitate H-mode access. More regular boronizations which occur throughout a run campaign seem to have a less substantial effect on P_{L-H}. However, quantitative analysis of the boronization effect on power threshold is lacking. Wall conditioning in JET with the ILW appears to be less critical to plasma startup and H-mode formation, even following long shutdowns. This improves upon the JET experience with C PFCs, when more regular wall conditioning was required.

3.7 Summary

Combining results from all three devices yields the key finding of this section: ITER is not expected to have more challenging access to H-mode with a full W divertor than it would have with a C divertor. This is largely based on comparisons among devices of H-mode power threshold, P_{L-H}, in D plasmas, and comparisons on single devices of P_{L-H} in D vs. He plasmas. Experiments comparing P_{L-H} in D and He plasmas in JET, with its ITER-like wall, would be extremely valuable in making these conclusions firmer.

References

[Ryter 2002] F. Ryter *et al.* Plasma Phys. Control. Fusion **44** (2002) A415.

[Lipschultz, 2006] B. Lipschultz *et al.* Phys. Plasmas **13** (2006) 056117.

[Neu 2007] R. Neu *et al.* J. Nucl. Mater. **363—365** (2007) 52.

[Ryter 2009] F. Ryter *et al.* Nucl. Fusion **49** (2009) 062003.

[Neu 2013] R. Neu *et al.* J. Nucl. Mater. (2013) in press.

[Ryter 2013] F. Ryter *et al.* Nucl. Fusion , submitted.

[Andrew 2006] Y. Andrew *et al.*, PPCF **48** (2006) 479.

[Maggi 2012] C. Maggi, EPS 2012 O3-108

[Ma 2012] Y. Ma, *et al.* Nucl. Fusion **52** (2012) 023010.

[Gohil 2012] P. Gohil *et al.* IAEA FEC 2012. ITR/P1-36.

4. Operation in H-mode

4.1 Introduction

Present devices with high-Z PFC components have identified some requirements for a stable operation in H-mode, that is in order to keep heavy impurity concentrations sufficiently low (in general below 10^{-4}), avoid central accumulation and radiative collapses and disruptions. These requirements imply some limitations in the operational space which can be accessed in H-mode, which can be grossly described as the need of operating at sufficiently high levels of gas puff and therefore as the limitation to access low density regimes at low gas puff levels. The implications of these operational requirements on the confinement and the plasma performance will be discussed in Section 5.

The present understanding identifies the different nature of impurity transport in the edge region (mainly neoclassical in the H-mode pedestal, mainly turbulent in the L-mode edge) as the main difference in the confined plasmas between H-mode and L-mode. Moreover, stable H-mode operation is regularly characterized by the presence of ELMs (or, period relaxations of the edge transport barrier), which have additional effects on the overall behaviour of high-Z impurities. Therefore, a complete description of their behaviour during the operation in H-mode has to consider all the components of the transport chain which connects the divertor to the centre of the plasma. In this section, these components will be examined, starting from the erosion sources, then moving to the transport in the edge (pedestal) region, and finally to the transport in the central region. A complex set of interconnections between edge and core are identified, which imply that the behaviour of high-Z impurities, and in particular whether the core accumulation can be prevented, does not depend on a single parameter, but on a complex and highly nonlinear relationship between several different effects.

4.2 Erosion Sources

Due to the high threshold energy of the hydrogenic sputtering yield, erosion of W occurs mainly by impurity ions at the relevant temperatures (T_e<100eV) in the divertor [Thoma PPCF 1997, Dux JNM 2009, Kallenbach JNM 2011, Van Rooij JNM 2013]. In present devices, erosion in the divertor is often dominated by the sputtering during ELMs [Van Rooij JNM 2013, Dux JNM 2009]. In between ELMs, elevated divertor temperatures may cause considerable W-erosion during the inter-ELM phases leading to about equal contributions of the inter-ELM and intra-ELM sputtering [Dux JNM 2009], however, in partially detached plasmas, which are required in ITER, the sputtering during ELMs strongly dominates due to the strongly increased sputtering yield [Neu JNM 2011, Kallenbach JNM 2011]. Generally, the W-source is well screened by the divertor plasma [Thoma PPCF 1997, Geier PPCF 2002, Pütterich IAEA 2012]. There are indications that the W-source at the baffles, i.e. at the entrance of the divertor, has a stronger impact on the W-content of the plasma than the larger source located directly in the divertor [Lunt JNM 2011].

For ASDEX Upgrade (AUG), it was found that the tungsten sources at the outboard limiters

have the strongest influence on the tungsten density in the confined plasma [Dux JNM 2009], such that a transfer of AUG results onto ITER where the source is solely located in the divertor area is difficult. In this respect, the results of W confinement studies from JET H-Mode operation [Pütterich IAEA 2012] are more relevant since the fraction of W PFCs in the main chamber of the ILW in JET is just one third. Results from Alcator C-Mod operations with a row of W tiles in the divertor with full Mo are also be relevant [Lipschultz – 2012].

For ITER plasmas, the divertor plasmas between ELMs are required to be detached or at least at temperatures in the range of a few eV. In order to obtain these low divertor temperatures impurity seeding accompanied with deuterium puffing is necessary. At divertor temperatures above a few eV the puffed impurities may increase the W-source, however, it has been shown at JET and AUG that sufficient radiative cooling by nitrogen overrules the detrimental effects by reducing the temperatures and the sputtering yield [Van Rooij JNM 2013, Kallenbach JNM 2011]. Alcator C-Mod also observes monotonic reduction of core molybdenum with increased low-Z impurity puffing using both neon and nitrogen [Reinke – 2012].

An important ingredient in the transport chain from divertor to main plasma is the prompt re-deposition of W [Naujoks NF 1996], i.e. the local deposition of W during the first gyro orbits. This effect is hard to quantify experimentally from direct measurements of gross and net erosion, i.e. by spectroscopic measurements of WI and WII lines [Brezinsek PS 2011, Van Rooij JNM 2013] or by comparison of spectroscopic gross erosion data versus net erosion from surface analysis [Dux JNM 2009]. However, the analysis of deposition patterns around W markers [Naujoks JNM 1994, Brooks NF 2013] or W tiles yield that this effect must exist and is significant, e.g. [Brooks NF 2013] finds 90% re-deposition in C-Mod. The effects on W re-deposition can be very significant in ITER. For the expected divertor conditions in H-modes between ELMs with high plasma density (~10^{20} - 10^{21} m^{-3}) and low plasma temperature (2-5 eV), which are required for divertor power load control, the proportion of W which is locally deposited after its first gyro-orbit is expected to be more than 80-90%. For the plasma conditions during the ELMs, where the electron temperature raises to at least 100's of eV, the amount of promptly re-deposited W even increases due to the large potential drop in the electric and magnetic sheath and the spatial extent of the sheath region. For the expected temperatures the potential drop is much larger than the mean energy of the sputtered W and the prompt re-deposition increases towards 100% [Chankin PC 2013].

4.3 Edge transport

Analyses of the transport in the H-mode edge pedestal show, that impurity transport is characterized by suppressed diffusion and, typically, a strong inward convection [Perry NF 1991, Pasini PPCF 1992, Pedersen NF 2000, Dux FST 2003, Pütterich JNM 2011]. Detailed measurements on helium, carbon, neon, and argon in type-I ELMy H-modes at AUG revealed, that the transport levels between ELMs are at or close to neoclassical levels and that the ratio of drift velocity to

diffusion coefficient increases with impurity charge [Pütterich JNM 2011]. Thus, W experiences a strong inward pinch at the H-mode pedestal resulting in steeper W-density profiles than electron density profiles.

A dosed efflux of impurities is necessary to provide an acceptable impurity level inside of the edge transport barrier. H-mode operation at JET and AUG showed, that elevated ELM frequencies are beneficial for the impurity control, as the additional impurity source is of lower importance for the W-content in the confined plasma than the impurity flushing by the ELMs [Dux NF 2011, Pütterich IAEA 2012]. The ELM frequency, which is required to effectively control the W peaking in the edge pedestal, depends on the characteristic equilibration time for the W profile which in turn is determined by the neoclassical transport coefficients. The neoclassical transport coefficients in the ITER ETB are estimated to be very small (ITER reference at 15MA/5.3T has about a factor of 30 lower diffusion coefficient ($D=0.01 m^2/s$) than in typical AUG H-mode plasmas at 1MA/2.5T) [Dux NF 2011], such that even low ELM frequencies on the order of 15Hz are sufficient to keep the W concentration at acceptable levels [Loarte IAEA 2012]. Here, the control of the power exhaust requests an even higher ELM frequency around 30-40 Hz [Loarte IAEA 2012]. Plasmas with lower current and toroidal field (7.5MA/2.65T) have roughly three times higher neoclassical diffusion coefficient, but the required ELM frequency is again estimated to be about 15Hz due to the lower erosion source, while power exhaust requirements are estimated to be compatible with uncontrolled ELMs. Since the uncontrolled ELM frequency is estimated to be ~3 Hz in 7.5MA/2.65T plasmas, ~5 times higher ELM frequency will be required for steady H-mode operation. Full ELM suppression using RMP coils is also planned for ITER and consequences for high-Z transport in the pedestal with RMP needs further study.

Present studies dedicated to the prediction of the neo-classical pinch direction in the H-mode barrier for detached or partially detached H-mode operation in ITER suggest that this might be in the outward directed. Acceptable power loads to the divertor ($\leq$ 10 MWm^{-2}) in Q=10 conditions are expected to require rather high separatrix densities in excess of $3\times10^{19} m^{-3}$ [Kukushkin 2012], while for the 7.5 MA/2.65 T H-mode a separatrix density of $1.5\text{-}2.0\times10^{19} m^{-3}$ [Kukushkin 2010] is compatible with an acceptable divertor power load. At the same time, the pedestal temperatures need to be high to reach the Q=10 goal. Thus, the normalised ion temperature gradient is usually more than two times the normalised density gradient and the temperature screening term dominates the neo-classical drift velocity, which is then outward directed [Dux EPS 2013]. This mode of operation with large pedestal temperatures and at the same time large densities at the separatrix is not achieved in present day tokamaks. The present simulations yield for both cases, i.e. 15MA/5.3T (Q=10) and 7.5MA/2.65T (non-nuclear phase), an outward directed drift velocity of W for the separatrix densities required by the control of the power load [Dux EPS 2013]. Under such conditions, impurity flushing by ELMs is not needed to keep the tungsten concentration at low levels. Thus, the previously described ELM

frequency requirements to suppress the W peaking in the H-mode barrier might not apply in ITER.

4.4 Core transport

Observations in H-mode plasmas show that impurity diffusion coefficients can be small and can even approach neoclassical levels in the central region of the plasma [Dux PPCF 03, Giroud ITPA 2010, Howard PoP 2012]. Therefore, the neoclassical convection can become significant, and can lead to central impurity accumulation, in the presence of centrally peaked density profiles. W accumulation must be avoided for stable plasma operation, as an increased W-density in the plasma core leads to radiative losses reducing the electron temperatures and their gradients. A way which has been proven to avoid accumulation is central electron heating [Dux PPCF 03, Neu JNM 2003, Valisa NF 11]. The physical interpretation of this control method is that central heating is observed to significantly increase the diffusive component of the transport [Dux PPCF 03, Sertoli PPCF 11] and can balance the neoclassical convection, reducing the gradients in W-densities. In a few cases it has been shown that even an outward convection of anomalous type was achieved by central electron heating [Dux PPCF 03, Puiatti PoP 06, Valisa NF 11, Sertoli PPCF 11]. For Alcator C-Mod, auxiliary heated H-modes are maintained by core ICRF in sawtoothing plasmas and on-axis accumulation is not observed.

The impact of core electron heating on impurity transport has been subject of several studies also from the theoretical standpoint. In general, it has been shown that turbulent impurity transport is not predicted to lead to accumulation, since, in contrast to neoclassical transport, it does not involve mechanisms of inward convection which increase with increasing impurity charge [Angioni PoP 07, Camenen PoP 09]. Central electron heating has been also predicted to reduce the inward turbulent convection or even lead to outward convection [Angioni PRL 06], although agreement with the experimental observations has been found for AUG cases with ECRH [Angioni PPCF 07, Sertoli PPCF 11], but not on JET with ICRH [Puiatti PoP 06, Valisa NF 11]. Recently, the theory of high-Z impurity transport has been further developed, including also the effects of rotation [Camenen PoP 09, Casson PoP 10, Angioni PoP 12] and poloidal asymmetries induced by auxiliary heating systems [Fulop PoP 11, Mollen PoP 12], which have been also observed experimentally [Reinke PPCF 12]. Systematic and detailed quantitative comparisons of the theory predictions with experimental results of high-Z impurity transport have not been performed, but experiments have been performed and are currently being analyzed. However, at a general qualitative level, the empirical result that the increase of the turbulent component of the impurity transport with respect to neoclassical impurity transport prevents heavy impurity accumulation remains consistent with the theoretical predictions. In addition, first studies of detailed comparisons on low-Z impurity turbulent transport [Angioni NF 11, Howard NF 12, Casson NF 13] show reasonable quantitative agreement between theoretical predictions and experimental observations, a result which gives confidence on the applicability of the theory also to heavy impurities.

In contrast to central heating, core radiation produces a transport effect which is opposite. At sufficient levels it accelerates the accumulation, and can lead to increasingly strong accumulating states of the plasma. Therefore, a reduced source at the plasma edge (either by reducing the erosion source or by enhancing the screening of W at the plasma edge) has a similar effect in avoiding impurity accumulation as that of core heating. In fact, the radiation power density of W can have the same profile of central heating in case of accumulation, but can also be flat/hollow in the absence of accumulation, which is more favourable for operation. The effect of central radiation implies that the avoidance of impurity accumulation does not depend on a single parameter (or actuator), but is determined by the realization of a set of mutually dependent conditions, in which the behaviour in the core is not independent from that at the edge, as a consequence of a transport chain which connects the plasma facing components to the center of the plasma. While this prevents simple conclusions to be drawn on the requirements of central auxiliary heating to avoid accumulation, it suggests multiple techniques may be available to avoid the deleterious effects of elevated core impurity contamination.

Finally, the role of MHD modes has not been characterized in all detail yet. While a frequent occurrence of sawtooth crashes seems to avoid W accumulation, modes at mid-radius seem to facilitate core accumulation, as particularly observed in recent hybrid scenarios at JET [T. Hender, private communication 2013]. For strong W-accumulation also a feedback exists, which seems to suppress the sawteeth by radiative cooling.

4.5 Ion Cyclotron Resonance Heating (ICRH)

Among the possible heating systems to be applied for central heating and avoid W accumulation, ICRH offers a cheap (in $/MW) reliable mean of heating the plasma core. However, a strong increase of impurity content in H-mode plasmas is observed throughout the plasma when ICRH is used, reducing the positive effect of the heating [Wukitch JNM 2009, Bobkov NF 2010]. In AUG, the W limiters of the ICRH antenna imply large local W sources during ICRH [Dux JNM 2007, Bobkov NF 2010, Bobkov JNM 2011]. These, however, should not be expected in ITER, with Be limiters. In JET with the ILW and Be limiters, efficient plasma heating has been obtained. The ILW and ICRH are compatible as heat loads and impurity levels stay within acceptable limits without compromising the heating performance [Van Ester EPS 2012, Jacquet PSI 2012, Bobkov PSI 2012]. However increased W concentrations with respect to similar levels of power by NBI heating have been observed, which suggest that W PFCs located far from the ICRH antennas can still play a role [Mayoral IAEA 2012]. In the strike point area, no increased W influx due to ICRH was observed [Mayoral IAEA 2012]. One third of the main chamber PFC area is W coated in the ILW-JET and might be responsible for the increased W concentrations. Similarly on C-Mod, when thick boron coatings were applied to ICRF limiters and portions of the outboard limiter, Mo contamination remained an issue for H-mode plasmas sufficiently removed from a

boronization. The identification of the physical mechanisms by which remote, possibly recessed, high-Z surfaces can produce impurity sources in the presence of ICRH is presently under study on multiple devices.

Certain measures like replacing high-Z limiters by boron-coated ones are used in present experiments with full high-Z walls to make use of ICRH, but a reactor-relevant solution with all high-Z wall requires an improved design of the antennas, which minimizes the impurity source [Bobkov NF 2010, Bobkov IAEA 2012, Wukitch IAEA 2012]. In contrast, normal antenna designs can be expected to be compatible with the ITER wall, with Be limiters and a W divertor.

4.6 Interconnection of the different plasma regions

As we already mentioned, there are several processes which are directly interconnected and which determine the behaviour of W in H-mode plasmas. Therefore the W behaviour has to be regarded as a highly nonlinear transport chain which connects the wall to the plasma core. The edge source impacts the concentration levels, which impact the radiation levels and the effective core heating power, which affects the properties of the W transport in the core. At the same time, core radiation impacts the heat flux all along the minor radius and to the wall. By this, not only it impacts the transport properties in the core, but also those at the edge, as well as the ELM frequency. Finally an increase of core and edge radiation can lead to a reduction of the W source by reducing the heat fluxes and the temperatures at the plasma facing wall components.

4.7 Discussion

It should be noted that even though the experiences in Alcator C-Mod, AUG and JET are encouraging, uncertainties remain for reliable quantitative predictions, since, as clarified in this section, the prediction of whether certain operation conditions will lead to accumulation depends on a highly nonlinear interconnection of various physics processes, some of which are even not appropriately individually described by present models (a very common issue for several physics aspects in ITER). The uncertainties in the predictions for the W content in the plasma are situated mainly in the plasma edge and in the most central region of the plasma.

In the edge, the plasma recycling fluxes and the spatial distribution of the local ion and electron temperatures govern the erosion locations and determine the eroded quantities. The penetration of the eroded W flux depends on the flows structure in the scrape-off layer and the divertor as well as on the radial transport across the separatrix and in the edge region. Small differences in erosion location might change the penetration of the eroded W significantly. All these elements can be predicted with a limited accuracy for ITER. In the core, the exact interplay between neoclassical transport and turbulent transport, with the inclusion of parallel transport effects which can become significant for high-Z impurities, provide a challenge to quantitative predictions. Finally, MHD activity (in both central and more peripheral plasma regions) can also be an important ingredient in some conditions, but not all the mechanisms by which MHD modes can impact the W confinement

have been clarified yet.

4.8 Summary

From present experiments, in particular AUG with full W wall, JET with the ILW and Alcator C-Mod with Mo wall, experience with high-Z wall materials exists that allows us to draw some conclusions on the impact of a W-divertor on the operation in H-mode discharges in ITER.

The recipes that have been developed in Alcator C-Mod, AUG and JET, for controlling the heavy impurity content of the plasma are the maximization of local core heating, the control of the impurity penetration by ELM pace-making, deuterium puffing and the mitigation of erosion by impurity seeding. These recipes are expected to be effective also in ITER to ensure stable H-mode operation. Thus, the large mix of different heating systems, fuel and impurity gas valves and means of ELM control can be expected to allow successful H-mode operation also in ITER, in the nuclear and the non-nuclear phase. More specifically, in the non-nuclear phase, the early availability of the ECH system is recommended, since it has been proven to be a very effective tool.

References

[Thoma PPCF 1997] A. Thoma et al., Plasma Phys. Control. Fus. 39 (1997) 1487.

[Dux JNM 2009] R. Dux et al., J. Nucl. Mater. 390-391 (2009) 858.

[Kallenbach JNM 2011] A. Kallenbach et al., J. Nucl. Mater. 415 (2011) S19-S26.

[Van Rooij JNM 2013] G.J. van Rooij et al., J. Nucl. Mater. (2013) in press.

[Geier PPCF 2002] A. Geier et al., Plasma Phys. Control. Fus. 44 (2002) 2091.

[Pütterich IAEA 2012] T. Pütterich et al., IAEA-CN-197/EX/P3-15 (2012).

[Lipschultz NF 2012] B. Lipschultz et al., Nucl. Fus. 52 (2012) 123002.

[Reinke PC 2013] M. Reinke, priv. comm. (2013).

[Neu JNM 2011] R. Neu et al., J. Nucl. Mater. 415 (2011) S322.

[Lunt JNM 2011] T. Lunt et al., J. Nucl. Mater. 415 (2011) S505.

[Naujoks NF 1996] D. Naujoks et al, Nucl. Fus. 36 (1996) 671.

[Brezinsek PS 2011] S. Brezinsek et al, Phys. Scr. T145 (2011) 014016.

[Naujoks JNM 1994] D. Naujoks et al, J. Nucl. Mater. 210 (1994) 43.

[Brooks NF 2013] J.N. Brooks et al, Nucl. Fusion 53 (2013) 042001.

[Chankin PC 2013] A.V. Chankin et al, priv. comm. (2013).

[Perry NF 1991] M.E. Perry et al., Nucl. Fusion 31 (1991) 1859.

[Pasini PPCF 1992] D. Pasini et al., Plasma Phys. and Contr. Fusion 34 (1992) 677.

[Pedersen NF 2000] T.S. Pedersen et al., Nucl. Fusion 40 (2000) 1795.

[Dux FST 2003] R. Dux, Fusion Science and Techn. 44 (2003) 708.

[Pütterich JNM 2011] T. Pütterich et al., J. Nucl. Mater. 415 (2011) S334.

[Dux NF 2011] R. Dux et al., Nucl. Fusion 51 (2011) 053002, 119501.

[Pütterich IAEA 2012] T. Pütterich et al., IAEA-CN-197/EX/P3-15 (2012).
[Loarte IAEA 2012] A. Loarte et al., IAEA-CN-197/ITR/1-2 (2012).
[Kukushkin IAEA 2012] A. Kukushkin, et al., IAEA-CN-197/ITR/P1-27 (2012).
[Kukushkin IAEA 2010] A. Kukushkin, et al., IAEA-CN-197/ITR/P1-33 (2012).
[Dux EPS 2013] R. Dux et al., EPS-Conf., Helsinki (2012) P4.143, to appear.
[Dux PPCF 2003] R. Dux et al, Plasma Phys. Control. Fusion 45 (2003) 1815.
[Giroud ITPA 2010] C. Giroud et al, ITPA Mtg, Culham 2010.
[Neu JNM 2003] R. Neu et al, J. Nucl. Mater. 313 116 (2003).
[Sertoli PPCF 2011] M. Sertoli et al, Plasma Phys. Control. Fusion 53 (2011) 035024.
[Valisa NF 2011] M. Valisa et al. Nucl. Fusion 51 (2011) 033002.
[Puiatti PoP 2006] M.E. Puiatti et al, Phys. Plasmas 13 (2006) 042501.
[Angioni PoP 2007] C. Angioni et al, Phys. Plasmas 14 (2007) 055905.
[Camenen PoP 2009] Y. Camenen et al, Phys. Plasmas 16 (2009) 012503.
[Angioni PPCF 2007] C. Angioni et al, Plasma Phys. Control. Fusion 49 (2007) 2027.
[Casson PoP 2010] F.J. Casson et al, Phys. Plasmas 17, 102305 (2010).
[Angioni PoP 2012] C. Angioni et al, Phys. Plasmas 19, 122311 (2012).
[Fulop PoP 2011] T. Fulop and S. Moradi, Phys. Plasmas 18, 030703 (2011).
[Mollen PoP 2012] A. Mollen et al, Phys. Plasmas 19, 052307 (2012).
[Reinke PPCF 2012] M.L. Reinke et al, Plasma Phys. Control. Fusion 54, 045004 (2012).
[Angioni NF 11] C. Angioni et al, Nucl. Fusion 51, 023006 (2011).
[Howard NF 12] N. T. Howard et al, Nucl. Fusion 52, 063002 (2012).
[Casson NF 13] F.J. Casson et al, Nucl. Fusion to be published (2013).
[Wukitch JNM 09] S. J. Wukitch et al, J. Nucl. Mater. 390-391 (2009) 951.
[Bobkov NF 10] V. Bobkov et al, Nucl. Fusion 50 (2010) 035004.
[Dux JNM 07] R. Dux et al, J. Nucl. Mater. 363-365 (2007) 112-116.
[Bobkov JNM 2011] V. Bobkov et al, J. Nucl. Mater. 415 (2011) S1005-S1008.
[Van Ester EPS 2012] D. Van Ester et al, EPS Conf. Plasma Physics 2012.
[Jacquet PSI 2012] P. Jacquet et al, Int. Conf. PSI 2012, P1-020.
[Bobkov PSI 2012] V. Bobkov et al, 20th Int. Conf. PSI 2012, O3.
[Mayoral IAEA 2012] M.-L. Mayoral et al, IAEA-CN-197 (2012).
[Bobkov IAEA 2012] V. Bobkov et al, IAEA-CN-197 (2012), EX/P5-19.
[Wukitch IAEA 2012] S.J. Wukitch et al, IAEA-CN-197 (2012).

5. Quality of H-mode plasmas

5.1 Introduction

The change over from a full carbon to a full metal wall has reduced the accessible operational space in both ASDEX Upgrade (AUG) and JET tokamaks. The AUG carbon wall (AUG-C) was replaced in a step wise manner from 1999 to 2007 by a DEMO-relevant full W-wall and divertor (AUG-W) [1], whereas in JET the carbon wall (JET-C) was fully replaced in 2009-2010 by an ITER-like Be main chamber first wall and W divertor (JET-ILW) [2].

5.2 Overall observations

We have found a common pattern in these full metal devices that the global and pedestal confinement are affected by a requirement for increased gas fuelling (to screen high-Z impurities influxes). Figure 5.1 shows a comparison of Type I ELMy H-mode plasmas in AUG (I_p=1MA, B_T=2-3T, δ=0.2, P_{In} = 3-6 MW, 1.3 < β_N < 1.6) [3]. The figure shows that for AUG-W the lower performance is correlated with high density and elevated fuelling level.

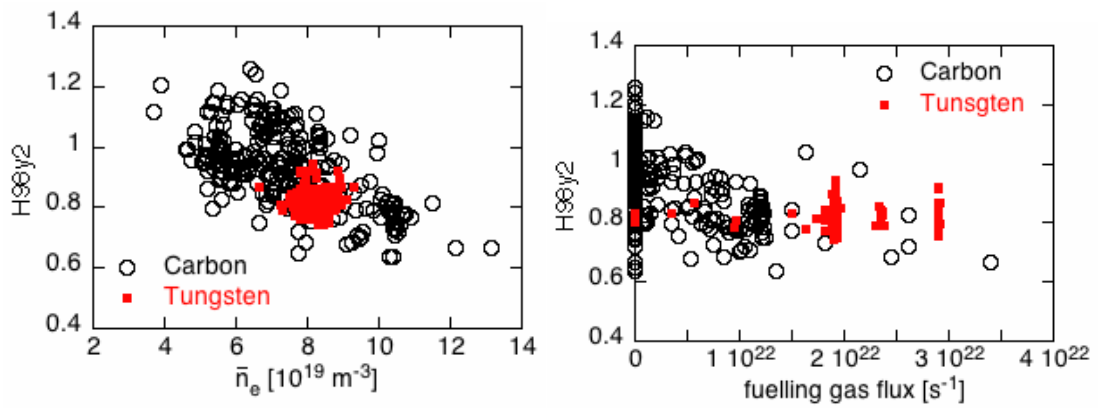

Figure 5.1 *AUG Database comparison of normalised confinement in 'standard H-modes' for operation with carbon (black) and Tungsten (red) wall. (Left) $H_{98y,2}$ vs line averaged density and (Right) $H_{98y,2}$ vs deuterium fuelling.*

In comparison, figure 2 shows the confinement for JET Type I ELMy H-mode plasmas (I_P =2.4-2.6 MA, B_T = 2.3-2.7 T, δ_{av}=0.2 and 0.4, P_{NBI} = 12-16 MW, 1.3 < β_N < 1.8). For low triangularity (δ) plasmas, the downward trend of $H_{98y,2}$ with density follows a similar trend as was reported for JET-C in [4] and is in agreement with the AUG observations. However, for the high-δ plasmas a further degradation is observed; whereas in JET-C high δ plasmas could sustain good confinement $H_{98y,2}$~1 up to the Greenwald density limit, the benefit of δ seems to have disappeared in JET-ILW [5,6].

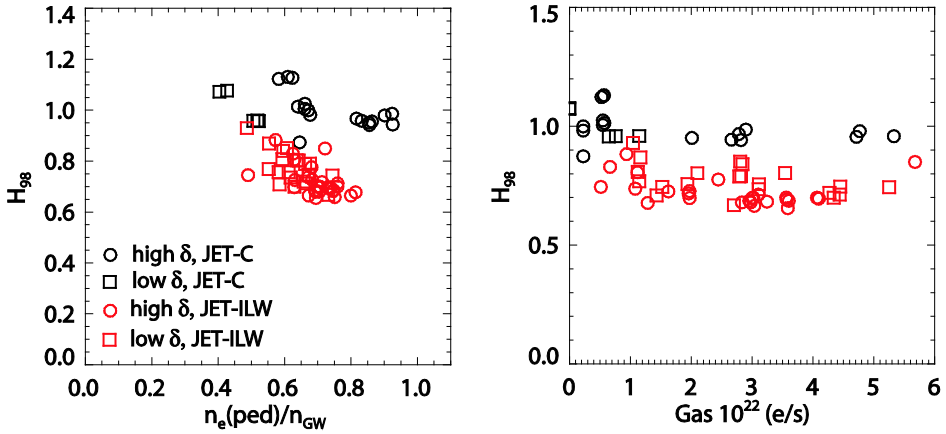

Figure 5.2 *JET database comparison of H_{98} for baseline Type I ELMy H-mode plasmas at low (δ=0.2) and high (δ=0.4) triangularity. (I_P =2.4-2.6 MA, B_T = 2.3-2.7 T, P_{NBI} = 12-16 MW)*

In AUG a strong correlation is found between the divertor neutral background pressure and normalised confinement in both AUG-C and AUG-W as can be seen in figure 5.3. It is so-far unknown in which way the divertor neutral pressure can affect the confinement. Nevertheless, in AUG-W this effect can be mitigated by means of impurity seeding as is demonstrated in figure 5.4, which compares two pulses with and without nitrogen seeding. The introduction of nitrogen in this case leads to a 10-15% increase in plasma stored energy and normalized confinement factor. At t=2.5s nitrogen is seeded and the normalised confinement increases from $H_{98y,2}$=0.8 to 1.2 whereas the divertor neutral pressure remains unchanged or even increases. A similar observation holds for JET. Here no divertor neutral pressure measurements are available and the divertor recycling level is used instead. Figure 5.5 shows $H_{98y,2}$ as a function of the inter-ELM outer-divertor D_α level (averaged over 20-80% of the ELM cycle). At increasing recycling level the normalised confinement steadily decreases for plasmas without nitrogen

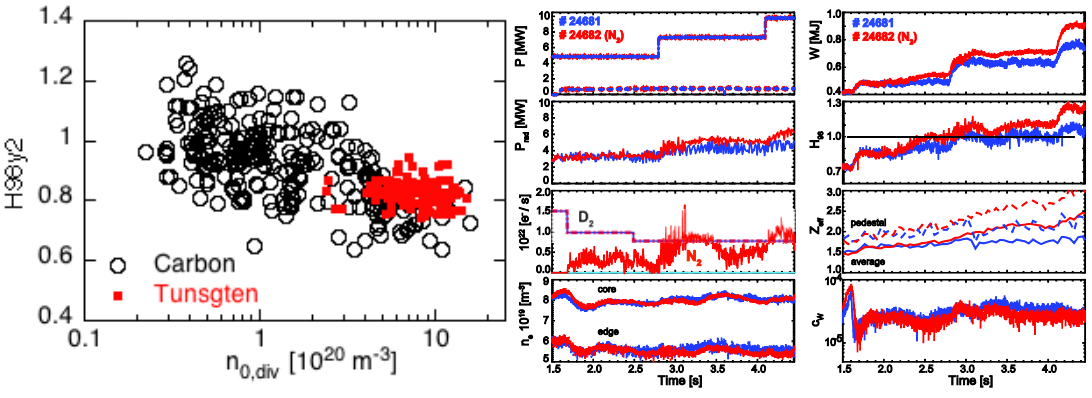

Figure 5.3 *(Left). AUG normalised confinement versus divertor neutral pressure.*
Figure 5.4 *(Right). Influence of Nitrogen seeding on confinement in AUG for I_p=1MA, B_T=2.5T. Pulse 24681 without seeding and pulse 24682 with nitrogen seeding,*

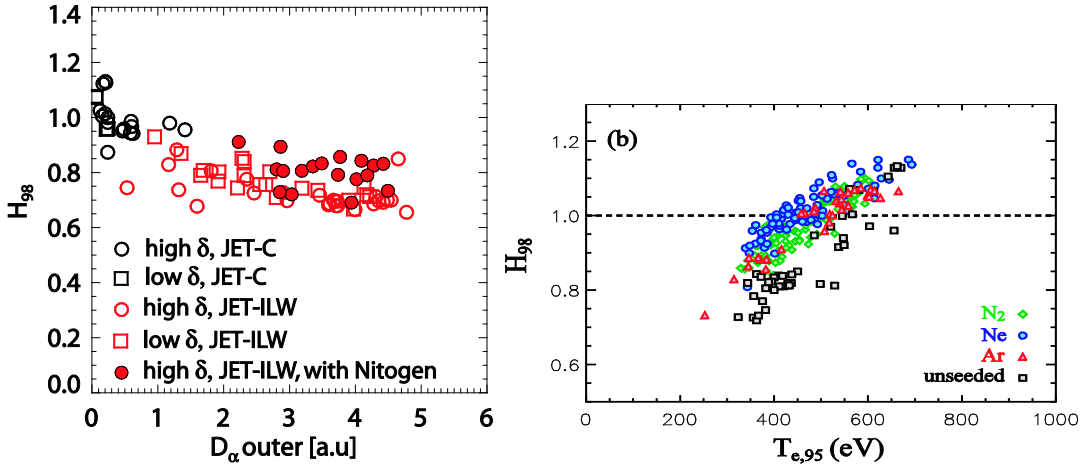

Figure 5.5 *(Left). JET normalised confinement versus inter-ELM D_α emission in the outer divertor averaged over 20-80% of the ELM cycle. Additional points are with N_2 seeding.*
Figure 5.6 *(Right). Improved confinement through impurity seeding in Alcator C-mod with a Molybdinum wall.*

seeding. However, like the AUG observations, when N_2 seeding is applied, $H_{98y,2}$ increases by up to 15%, approaching the enhancement factor obtained in JET-C. This beneficial effect of impurity seeding on plasmas confinement has also been observed in Alcator C-mod [7], figure 5.6, and is a general observation in tokamaks with a metal first wall. Moreover, in JET-C nitrogen seeding did not lead to an increase in confinement, which suggests that the low-Z impurities N_2 and C play a similar role in enhancing the plasmas confinement [8,9].

The global confinement improvement with N_2 seeding in JET-ILW is due to an enhancement of the pedestal pressure through an increase of the pedestal temperature [5,6], figure 7(a). The ratio of core and pedestal confinement remains unchained for all

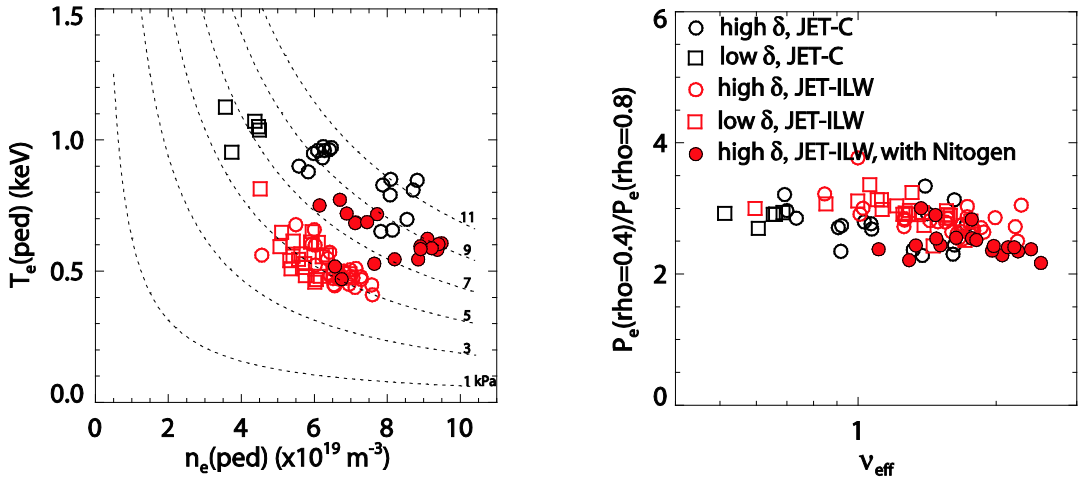

Figure 5.7 *(Left, a) JET Pedestal T_e and n_e diagram and (Right, b) JET pressure profile peaking for pulse selection as figures5. 2 and 5.5.*

the JET-C and JET-ILW pulses, as seen in Figure 7(b), and hence the confinement is set by the achievable pedestal pressure and profile stiffness. This has also been observed in AUG where N_2 leads to an increase in pedestal temperature and the core pressure profile peaking remains unchanged [10,11]. In contrast, for Alcator C-mod the confinement improvement is observed to be through an increase in pedestal density, although here also the core profiles are stiff.

5.3 Summary

In view of our recommendations for ITER, the clearest difference seen between full Carbon and full metal devices is the loss of the well performing zero gas flux, low recycling scenario going from C to W or Be/W, especially for initial operation phase in ITER. However, in Q=10 scenario with high gas rates and/or pellet injection for heat load mitigation and for operation close to the density limit, this is of little consequence for the choice in divertor material. The use of low-Z impurity seeding may aid the baseline H-mode scenario in ITER with a full metal wall, especially for the high-δ plasmas. This is in good synergy with the need for divertor heat load mitigation.

It is uncertain that an ITER scenario developed with low power in a CFC/W divertor can be transferred to an all-W ITER divertor. The uncertainties are obvious from the unexplained empirical behaviour shown here, and a clear recommendation is to work on the physics behind these observations. However, once CFC/W divertor is used in ITER, the entire wall will be contaminated with carbon. The concern of introducing CFC as a divertor material is that the presence of carbon as a low-Z impurity may alter plasma performance (like N_2 in all metal devices discussed here). This in turn may lead to the wrong estimate of the plasma performance in the nuclear phase of ITER operation where C as a divertor material is prohibited, which can be a merit of starting with a full W divertor.

References

[1] R Neu et al 2009 Phys. Scr. 2009 014038 doi:10.1088/0031-8949/2009/T138/014038

[2] [Matthews-PSI-2012] International Conference of Plasma Surface Interaction, Aachen, 2012

[3] F Ryter – Private communication

[4] G. Saibene et al, 2002 Plasma Phys. Control. Fusion 44 1769

[5] C Giroud et al, IAEA, 2012

[6] M Beurskens et al, IAEA, 2012

[7] A. Loarte et al, , Physics Review Letters, 2010

[8] G Madison et al, Physics Review Letters, 2011 &

[9] C Giroud et al, Nuclear fusion, 2012

[10] "Overview on plasma operation with a full tungsten wall in ASDEX Upgrade" Journal of Nuclear Materials In press, corrected proof, 0 (2013), doi:10.1016/j.jnucmat.2013.01.006

[11] G Tardini et al 2013 Plasma Phys. Control. Fusion 55 015010 doi:10.1088/0741-3335/55/1/015010

6. Specific issues in He plasma operation

6.1 Introduction

In order to commission the tokamak while maintaining physical accessibility, ITER will operate in a pre-nuclear phase with the fuel species being H and/or He. While the choice has yet to be decided, operation in He has been observed to have a lower L-H threshold power, P_{L-H}, on current devices as compared to H [Gohil – 2012]. This increases the likelihood that dominantly He plasmas will be used to investigate high performance scenarios in the pre-nuclear phase. Due to the observed increase of the threshold power with magnetic field, operation at ½-field (B_t=2.65 T, I_p=7.5 MA), is thought to be the most likely pre-nuclear operating point [Polevoi – 2011].

In Section 6.2, the L-H transition threshold, ELM physics and divertor impurity sources in He plasmas are briefly discussed. High-Z impurity transport is considered in Section 6.3. Previous studies in Ohmic L-mode plasmas dedicated to the scaling of the impurity confinement time with the background ion mass and charge and charge are reviewed. Uncertainties in these results motivate near-term experiments on tokamaks to better understand the physics impact of changing the main-ion species. In H-mode operation, W accumulation can be controlled through a complex interplay among different actuators, particularly the ELM frequency at the edge and localized heating in the core, as reported in Section 4. Experiments are presently planned to directly compare D and He plasma discharges with the ITER baseline scenario in the full W device ASDEX Upgrade (AUG).

6.2 Differences in Tokamak Operation

High power, diverted tokamaks such as JET [Behringer – 1989, Philipps – 2001, McDonald – 2004, 2010], AUG [Neu – 2008, Ryter – 2009], DIII-D [Gohil – 2010, 2011] and Alcator C-Mod [Snipes - 2010, Hughes - 2011] have been operated in helium within the last decades. Many of these experiments express common challenges such as maintaining particle control due to changes in recycling and difficulties in pumping He with cryopumps. For ITER the former will still be present, while charcoal-based cryopump panels will enable efficient He pumping in ITER. Change-over of plasma content from D to He generally takes a few discharges, but is sensitive to equilibrium shifts that can liberate new sources [Phillips – 2001]. Of particular concern when interpreting results from multiple devices, or devices over time, is accounting for the influence of wall material. For carbon machines (DIII-D and the JET results listed above), chemical sputtering normally present when using hydrogenic fuels does not occur in He plasmas, making comparisons at matched engineering parameters difficult to interpret due to qualitative changes in impurity source physics.

The dependence of the L-H power threshold was recently studied under joint experiment TC-4, reviewed in [Gohil – 2012] and is also discussed in Section 2. The threshold was measured in both deuterium and helium plasmas with a wide variety of auxiliary heating tools. Multi-machine experiments revealed $1.0 < P_{L-H,He}/P_{L-H,D} < 1.5$, with a density dependence that decreased the ratio as n_e was raised. In the full W device AUG a ratio $P_{L-H,He}/P_{L-H,D}$ around unity has been found [Ryter –

2009], in contrast to considerably larger values, around 1.4, in the C device DIII-D [Gohil – 2011]. At the same time, the Alcator C-Mod, with all molybdenum PFCs, observed similar trends as DIII-D. In both AUG and DIII-D, however, $P_{L\text{-}H,He}/P_{L\text{-}H,D}$ remains significantly below $P_{L\text{-}H,H}/P_{L\text{-}H,D}$, which is observed to be around 1.8 in both devices. Further study has been recommended, particularly including JET with the ILW, to try to better understand the cause of the different observations of $P_{L\text{-}H,He}/P_{L\text{-}H,D}$, reducing uncertainty for pre-nuclear scenario planning. Additional concerns lie in the increased L-H threshold power in plasma with both He and H. In the pre-nuclear phase, if ITER is unable to fuel with gas puffing alone, hydrogen pellets will be required. Recent results on AUG, shown in figure 6.1, reveal increased $P_{L\text{-}H}$ as the He purity is reduced with H [Ryter -2013]

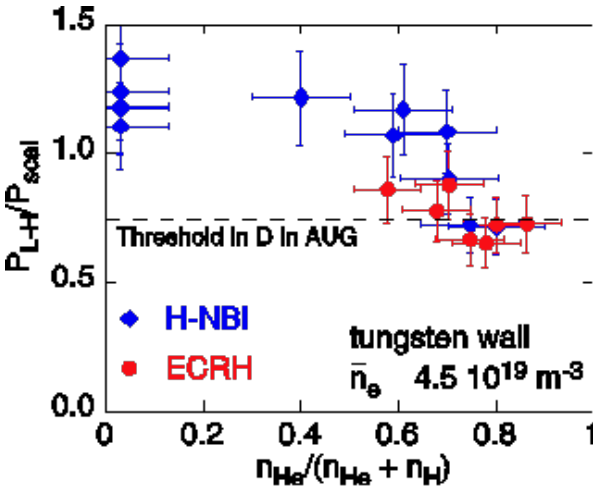

Figure 6.1 *Demonstration of increase in threshold in a mixed H/He plasma [Ryter-2013]*

Energy confinement has been shown to be worse in He plasmas, with $0.6 < \tau_{E,He}/\tau_{E,D} < 0.7$ when comparing similar discharges on JET [McDonald – 2004] and AUG [Ryter – 2009]. Results on AUG indicate this reduction occurs for very small levels of $n_{He}/(n_{He}+n_D)$, only a few percent, achievable as a by-product of standard He glow wall conditioning [Neu – 2009], while measurements on JET [McDonald – 2004] show a weaker degradation, with only a 10% reduction in H_{98} even up to $n_{He}/ne \sim 20\%$. The reduction in energy confinement in He has been ascribed to the reduction in ion pressure an fixed n_e [Ryter – 2009], and is distinct from the $m_i^{0.19}$ scaling in $\tau_{IPB98,y2}$ which was found only using hydrogenic plasmas. Both Type I and Type III ELMy H-modes have been accessed in for similar D and He plasmas in JET [McDonald – 2010] and AUG [Scarabosio – 2011]. Both plasmas show the same qualitative scaling with $P_{LOSS}/P_{L\text{-}H}$; a decrease in ELM frequency as normalized loss power is increased for Type III, transitioning to a mixed-regime and then an increasing Type I ELM frequency as $P_{LOSS}/P_{L\text{-}H}$ is raised. While ELM mitigation and/or suppression is not well studied for He plasmas, basic demonstration of concepts that work in deuterium plasmas have been shown to be successful [Suttrop – 2012]. At the end of the last AUG experimental campaign (April 2013) experiments have been performed to compare the ITER baseline scenario in D and He plasmas. While the analysis is still preliminary, these experiments allow us to draw some conclusions which are of relevance here. The operation of ITER baseline scenario in AUG with D requires central electron heating and sufficiently high levels of gas puff to avoid impurity accumulation. In contrast, in He plasmas (heated with D NBI) the operation of ITER baseline scenarios in AUG is possible even

without any central ECH, without any problem of W accumulation. The achieved density is close to the Greenwald density limit and the natural ELM frequency in these He plasmas is significantly higher than in the corresponding D discharges. Of course, also the confinement in He was observed to be much lower than in D [J. Schweinzer Priv. Comm. 2013 and EPS 2013].

Both JET and AUG show similar differences between He and D H-mode operations, suggesting the role of carbon (JET) or tungsten (AUG) PFCs is at most a secondary effect. Initial results from C-Mod demonstrated the transition from EDA to ELM-free H-mode in dominantly He plasmas was sensitive to purity level [Reinke – 2009], and that ELMy H-mode is accessible in both He and D plasmas [Hughes – 2011].

6.3 High-Z Impurity Transport

The use of He as a main-ion will lead to several changes which could raise core high-Z impurity concentrations, but the extent is unknown. The impurity source at regions of high particle flux will increase as a result of a reduced sputtering threshold [Kallenbach – 2007] and macroscopic flux could also be present due to breakdown or loss of "tungsten fuzz" [Wright – 2012]. Differences in ELM frequency will modify the rate at which high-Z impurities can be flushed out of the plasma [Dux – 2011]. Impurity transport in the core of enhanced confinement modes of different main-ions has not been systematically investigated to our knowledge. For deuterium plasmas in these regimes, on-axis peaking and accumulation of high-Z impurities is observed under certain conditions in both AUG and JET [Neu -2003, Joffrin IAEA FEC 2012], negatively impacting energy confinement and sustainment of the H-mode. In deuterium H-mode, control of W accumulation is routinely achieved in AUG by combining a sufficiently high frequency of the ELMs with central electron cyclotron heating [Neu - 2005, Kallenbach - 2009]. Core electron heating has been empirically demonstrated to counter-act this accumulation in deuterium plasmas as described in Section 4.

The present understanding allows us to conclude that the same effects of central electron heating on high-Z impurity transport can be expected in D, H and He plasmas. Although the precise

			Plasma Parameters			*Scaling Coefficients*		
DEVICE	**MAIN IONS**	**Impurity**	**ne [10^{20} m^{-3}]**	**Ip [MA]**	**Bt [T]**	**mi**	**Zi**	**Zeff**
TEXT	H,D, ^{4}He	Al	0.1-0.6	0.15-0.32	2.8	0.57	-0.57	1.16
Alcator C-Mod	H,D	various	-	-	-	0.23	x	x
TFTR	H,D,^{4}He	Ge,Cu,Ni,Ti,Mo	0.06-0.6	0.8-2.5	3.9-4.7	0	0	0
Alcator A	H,D, ^{3}He ^{4}He	Si	0.5-5.5	0.06-0.23	3.6-7.9	1	x	x
Alcator C	H,D,^{4}He	Al,Xi,Ti,Mo	0.5-6.8	0.1-0.7	3.5-12	1	-1	1
Tore Supra	D,^{4}He	Ni,Mn,Cu, Ge	0.1-0.4	0.8-1.7	2.6-4.0	0	x	0
JET	D,^{4}He	Si-Ti	0.1-0.43	2.0-7.0	1.5-3.5	0	x	0
TFR	H,D,^{4}He	V,Cr,Ni	0.6-1.2	0.2	4.5	1	x	x

Table 1: Machine-dependent scaling of impurity confinement time with main-ion, $\tau_z \sim m_i^a, Z_i^b, Z_{eff}^c$. An entry of 'x' in the last three columns implies this quantity was not considered in the scaling.

scaling of the required power in He plasmas in ITER remains uncertain, and can depend on several factors, He operation without core high-Z accumulation has been robustly reproduced in multiple devices. At this time, these observations remain at the level of "control-room analysis", and existing data could benefit from further scrutiny.

To gain more insight into the impact of an increased tungsten source for He main-ion Ohmic L-mode plasmas, impurity confinement data from a wide range of tokamaks has been assembled from previously published work. Multiple magnetic confinement devices have explored sensitivity of impurity transport to changes in the background ion species in these low confinement regimes. This has generally been done by studying the scaling of the impurity confinement time, τ_z, with background ion mass, m_i. Many also included Z_{eff} and Z_i, both of which change with main ion, while Z_{eff} can change independently due to other impurities. In most cases, impurities were introduced using a transient source via laser blow off (LBO) and the time constant of the exponential decay phase reported as τ_z. Table 1 summarizes the results described in the text.

The first experiments were completed on Alcator A [Marmar - 1980] and found substantial, systematic differences in Si confinement between H, D, ^{3}He and ^{4}He plasmas, with τ_z linearly increasing with m_i. Similar studies continued on Alcator C [Marmar - 1982] and a scaling for $\tau_z \sim m_i Z_{eff}/Z_i$ was derived using a wide operating range in H, D and ^{4}He plasmas. The TFR tokamak [TFR Group – 1982] also observed the linear scaling of τ_z with m_i for mid-Z impurities. On TEXT [Wenzel – 1989] Al confinement was measured in H, D and ^{4}He plasmas, and found to have a weaker scaling with the working gas species, $\tau_z \sim Z_{eff}^{1.16} m_i^{0.57} Z_i^{-0.57}$. Observations on Alcator C-Mod [Graf – 1995] also revealed a weaker dependence with $\tau_z \sim m_i^{0.23}$ when comparing H and D plasmas. In contrast, TFTR [Stratton – 1989] found no variation of impurity confinement time with main-ion species for a range of mid- to high-Z impurities, similar to studies completed on JET and Tore Supra [Mattioli – 1995]. The independence of τ_z with m_i in D and ^{4}He was also mentioned earlier for intrinsic Ni injections in JET [Behringer – 1989]. The reasons behind the wide variety of observations are not clear. This could be indicative of changes in the Ohmic confinement regime, i.e. linear to saturated Ohmic confinement, that since long has been interpreted as the consequence of a change in turbulence regime [Romanelli-1986, Angioni-2005, Rice – 2011, Angioni-2011]. While experiments are compared at the same engineering parameters, changing from D to He will change n_i/n_e, impact Ohmic heating for fixed I_p plasmas and directly change ρ_*, impacting micro-instability growth rates [Pusztai – 2011].

6.4 Summary

Several uncertainties still limit the possibility of making precise predictions in the definition of scenarios in the pre-nuclear operation phase of ITER in He. However, the present knowledge allows us to conclude that there is no specific element connected with operation in He plasmas by which it should be expected that pre-nuclear operation in He could be severely hampered or even made

impossible in the presence of a W divertor in ITER. Very recent (April 2013) experiments in AUG comparing the ITER baseline scenario in D and in He plasmas have shown that, in contrast to D discharges, in He discharges stable operation without W accumulation was possible even without any central ECH. One possible concern is an increase of hydrogen content in He plasma by hydrogen pellet injection for heavy impurity control, where the required power for L-H transition can be increased.

Appendix

With respect to core transport, we find there is nothing unique to operation in He that would significantly influence the decision for ITER to begin operations with a full tungsten divertor. But, there are sufficient uncertainties in core transport physics of He plasmas, specifically high-Z impurity transport, that may impact reliably designing pre-nuclear operational scenarios. We provide suggestions for near-term work to help mitigate this risk, helping to ensure successful operation of ITER.

Uncertainties still remain in answering very basic questions like the main-ion dependent scaling of L-H threshold and τ_z. Further analysis will be dedicated to the comparison of the ITER baseline scenario in D and He plasmas performed in AUG, which should help to obtain more information on the different requirements for stable operation in D and He plasmas. Longer term, we recommend further research to gain more understanding of m_i and Z_i dependent transport processes in order to reliably design pre-nuclear operational scenarios. Despite no open joint-experiments, in *any* ITPA topical group that focus on comparisons between H, D and He plasmas, it does not seem prudent to define new T&C joint experiments at this time. Instead, existing and planned experiments/activities should be used for scoping studies which can inform initial IOS decisions, which can then be used to frame appropriate joint experiments in all topical groups at some point in the future.

As mentioned in Section 6.2, the main-ion dependence of the L-H threshold has not yet been reliably settled, despite closing TC-4. Given the high-level priority of this topic, near-term run-time is anticipated. Therefore, we suggest, where possible, to included characterization of the impurity transport in plasmas with different main-ion species when revisiting these threshold experiments. This includes impurity studies for IOS 1.3: Operation near P_{L-H}, since this may generally characterize early ITER operation due to reduced auxiliary power as heating systems are deployed or a higher L-H threshold. Specific note should be taken of any differences in core electron heating power required to prevent on-axis high-Z impurity accumulation in H-modes. Extending TC-21 to include the study of multiple main-ion species and include impurity transport, especially τ_z using LBO, should be discussed. Alternatively, TC-11 studies on impurity transport could be extended to include He plasmas.

From the work done to complete this section, it is clear that while operation in He is nearly ubiquitous in tokamaks, operational capabilities may not translate from using H or D fuel. Specifically,

cryo-pumping and auxiliary heating can be very different, limiting the scope of proposed research. While ECH and hydrogen minority ICRH are essentially equivalent in D and ^{4}He plasmas, modification of neutral beam systems to run in different ions is facility dependent. We recommend that the ITPA, likely the IOS topical group, collect information on operational limitations (auxiliary heating, diagnostics, feedback control, etc.) with respect to main-ion species, including those projected for ITER. Making this data generally available to all ITPA groups will assist in defining future joint experiments that compare main-ion species. Additionally, the method of measuring main-ion purity varies, with some experiments using $n_{He}/(n_{He}+n_D)$ from core CXRS while others use ratios of D I and He I emission in the edge or divertor. Recommendations to standardize the helium fraction measurement would be helpful.

References

Angioni, C., *et al*. Phys. Plasmas **12**, 040701 (2005)

Behringer, K., *et al.* J. Nucl. Mater. **162-164** 298 (1989)

Dux, R., *et al*. Nucl. Fusion **51** 053002 (2011)

Gohil, P., *et al*. Nucl. Fusion. **50**064011 (2010)

Gohil, P., *et al.* Nuc. Fusion. **51** 103020 (2011)

Gohil, P., *et al*. Proc. of the 24th IAEA Fusion Energy Conference. ITR/P1-36 (2012)

Hughes, J.W., ELMy H-mode experiments in He and D

Joffrin, E., *et al*, 24th IAEA Fusion Energy Conference. EX/1-1 (2012)

Kallenbach, A., *et al*. Plasma Phys. Control. Fusion. **47** B207 (2005)

Kallenbach, A., *et al*. Nucl. Fusion **49** 045007 (2009)

McDonald, D.C., *et al*. Plasma Phys. Control. Fusion. **46** 519 (2004)

McDonald, D.C., *et al*. Proc. of the 23rd IAEA Fusion Energy Conference. EXC/2-4Rb (2010)

Mattioli, M., *et al.* Nucl. Fusion **35** 1115 (1995)

Marmar, E.S., *et al*. Phys. Rev. Lett. **45** 2025 (1980)

Marmar, E.S., *et al*. Nucl. Fusion **22** 1567 (1982)

Neu, R., *et al*. J. Nucl. Mater. **313** 116 (2003)

Neu, R., *et al*. Nucl. Fusion **45** 209 (2005)

Neu, R., *et al*. 35th EPS Conf. on Plasma Phys. **32D** P4.039 (2008)

Philipps, V., *et al*. 28th EPS Conf. on Contr. Fusion and Plasma Phys. ECA **25A** 1737 (2001)

Polevoi, A.R., *et al*. 38th EPS Conf. on Plasma Phys. P4.109 (2011)

Pëtterich, T., *et al*. J. Nucl. Mater. **415** S334 (2011)

Pusztai, I. *et al*. Phys. Plasmas. **18** 122501 (2011)

Reinke, M. "L-H threshold in mixed He and D plasmas" Alcator C-Mod Ideas Forum. #409 (2009)
http://www.psfc.mit.edu/research/alcator/program/ideas2009/Ideas09_mlreinke_lhthreshold.pdf

Rice, J.E., *et al*. Phys. Plasmas **19**, 056106 (2012)

Romanelli, F., *et al*. Plasma Phys. Control. Fusion **26** 1515 (1986)

Ryter, F., *et al*. Nucl. Fusion. **49** 062003 (2009)

Ryter, F., *et al*. 'Survey of the H-mode power threshold and transition physics studies in ASDEX Upgrade', submitted to Nucl. Fusion (2013)

Scarabosio, A., *et al*. J. Nucl. Mater. **415** S877 (2011)

Snipes, J., - L-H threshold experiment

Stratton, B.C., *et al*. Nucl. Fusion **29** 437 (1989)

Suttrop, W., *et al*. Proc. of the 24th IAEA Fusion Energy Conference. EXC/3-4 (2012)

TFR Group. Phys. Lett. **87A** 169 (1982)

Acknowledgements

The chairs of the T&C and PEP topical groups acknowledge all the topical group members who have contributed to this joint group activity through providing data, discussions and fruitful comments. In particular, the chairs are grateful to the authors of each section for their kind efforts in writing text, collecting results and analysis.

The authors of section 2 acknowledge S. Fietz, M. Groth, E. Joffrin, A. Kallenbach, K. McCormick, R. Neu, T. Püetterich, J.E. Rice, F. Ryter for very useful discussions and their contributions to section 2.

The authors of section 3 acknowledge P. Gohil, B. Lipschultz, Y. Ma, R. Neu, S. Wolfe for very useful discussions and their contributions to section 3.

The authors of section 4 acknowledge M. Reinke for his contributions to Section 4 and E. Joffrin, A. Kallenbach and R. Neu for very useful discussions.

The authors of section 5 acknowledge C. Giroud, J. Hughes, A. Kallenbach, P. Lomas, G. Maddison, R. Neu, I. Nunes for very useful discussions and their contributions to section 5.

The authors of section 6 acknowledge J.E. Rice and E.S. Marmar for discussions of early Alcator results. The work is supported in part by an appointment to US DOE Fusion Energy Postdoctoral Research Program administered by ORISE.